Interatomic collisions in a tightly confined Bose gas

D. S. Petrov[1,2] and G. V. Shlyapnikov[1,2,3]
[1]*FOM Institute for Atomic and Molecular Physics, Kruislaan 407, 1098 SJ Amsterdam, The Netherlands*
[2]*Russian Research Center, Kurchatov Institute, Kurchatov Square, 123182 Moscow, Russia*
[3]*Laboratoire Kastler Brossel,* 24 rue Lhomond, F-75231 Paris Cedex 05, France*
(Received 6 December 2000; published 5 June 2001)

We discuss binary atomic collisions in a Bose gas tightly confined in one (axial) direction and identify two regimes of scattering. In the quasi-two-dimensional (quasi-2D) regime, where the confinement frequency ω_0 greatly exceeds the gas temperature T, the scattering rates exhibit 2D features of the particle motion. At temperatures $T\sim\hbar\omega_0$ one has a confinement-dominated 3D regime, where the confinement can change the momentum dependence of the scattering amplitudes. We describe the collision-induced energy exchange between the axial and radial degrees of freedom and analyze recent experiments on thermalization and spin-relaxation rates in a tightly (axially) confined gas of Cs atoms.

DOI: 10.1103/PhysRevA.64.012706 PACS number(s): 34.50.−s, 05.30.Jp, 32.80.Pj

I. INTRODUCTION

Collisional properties of ultracold gases strongly confined in one direction attract a great deal of interest since the start of active studies of spin-polarized atomic hydrogen. In the latter case the interest was related to recombination and spin-relaxation collisions and to elastic scattering in the (quasi) two-dimensional (2D) gas of atomic hydrogen adsorbed on liquid-He surface (see [1] for review). The discovery of Bose-Einstein condensation in trapped alkali-atom clouds [2–4] stimulated a progress in evaporative and optical cooling and in trapping of neutral atoms. Present facilities make it possible to (tightly) confine the motion of particles in one direction to zero-point oscillations. Then, kinematically the gas is 2D, and the only difference from the purely 2D case is related to the value of the interparticle interaction that now depends on the tight confinement. Thus, one now has many more opportunities to create (quasi)2D gases. In the recent experiments with optically trapped Cs [5–8] about 90% of atoms are accumulated in the ground state of the harmonic oscillator potential in the direction of the tight confinement.

In this paper we consider a Bose gas tightly confined in one (axial) direction and discuss how the axial confinement manifests itself in pair elastic and inelastic collisions. We identify two regimes of scattering. At temperatures $T\ll\hbar\omega_0$ (ω_0 is the axial frequency) only the ground state of the axial harmonic oscillator is occupied, and one has a quasi-2D regime. In this case, the 2D character of the relative motion of particles at large separation between them, manifests itself in a logarithmic energy dependence of the scattering amplitude. For a negative 3D scattering length a, we observe resonances in the dependence of the elastic scattering rate on a. This is quite different from the 3D case where the scattering rate always increases with a^2. The presence of these resonances in quasi2D follows from the analysis given in [9] and finds its origin in increasing role of the 2D kinematics of the particle motion with increasing ratio $|a|/l_0$, where $l_0=(\hbar/m\omega_0)^{1/2}$ is the axial extension of the atom wave function, and m the atom mass.

At temperatures $T\sim\hbar\omega_0$ we have a confinement-dominated 3D regime of scattering, where the 2D character of the particle motion is no longer pronounced in the scattering process, but the axial confinement can strongly influence the energy (temperature) dependence of the scattering rate. Treating collisions as three dimensional, the wave vector p of the relative motion of colliding atoms does not decrease with T at $T\lesssim\hbar\omega_0$. The atoms undergo zero-point oscillations in the axial direction and this corresponds to $p\sim 1/l_0$. If the 3D scattering amplitude is momentum dependent at these p, which is the case for $|a|\gtrsim l_0$, then the temperature dependence of the elastic collisional rate becomes much weaker. This means that for a large 3D scattering length the tight axial confinement suppresses a resonant enhancement of the collisional rate at low energies. In many of the current experiments with ultracold gases one tunes a to large positive or negative values by varying the magnetic field and achieving Feshbach resonances [10–14]. In the unitarity limit ($|a|\to\infty$) the 3D elastic cross section is $\sigma=8\pi/p^2$ and the rate of 3D elastic collisions strongly increases with decreasing temperature. The tight confinement of the axial motion makes the scattering rate practically temperature independent at $T\sim\hbar\omega_0$. We obtain a similar suppression of resonances for inelastic collisions, where the resonant temperature dependence in 3D is related to the energy dependence of the initial wave function of colliding atoms. We analyze the Stanford and ENS experiments on elastic [6,8] and spin relaxation [6] collisions in a tightly axially confined gas of cesium atoms and discuss the origin of significant deviations of the observed collisional rates from the 3D behavior.

We develop a theory to describe the collision-induced energy exchange between axial and radial degrees of freedom of the particle motion. We establish selection rules for transitions between particle states in the axial harmonic potential and calculate the corresponding transition amplitudes. This allows us to consider temperatures $T\gtrsim\hbar\omega_0$ and analyze thermalization rates in nonequilibrium clouds. In the Stanford and ENS experiments these clouds were created by means of degenerate Raman sideband cooling [5–8] that effectively

*LKB is a unité de recherche de l'Ecole Normale Superieure et de l'Université Pierre et Marie Curie, associée au CNRS.

leads to a gas with different axial (T_z) and radial (T_ρ) temperatures. After the cooling is switched off, the temperatures T_z and T_ρ start to approach each other, and ultimately the gas reaches the equilibrium temperature. At sufficiently low T only a few axial states are occupied and the temperature dependence of the corresponding thermalization rates should deviate from the 3D behavior, thus exhibiting the influence of the axial confinement on the scattering process. We calculate the thermalization rates and establish the conditions under which this influence is pronounced.

The minimum energy exchange between the radial and axial degrees of freedom of two colliding atoms is equal to $2\hbar\omega_0$. This follows from the symmetry of the interatomic potential with respect to simultaneous inversion of the axial coordinates of the two atoms, which ensures the conservation of parity of their wave function under this operation. Accordingly, the sum of two (axial) vibrational quantum numbers can be changed only by an even value. The rate of energy transfer from the radial to axial motion is proportional to the difference between the radial and axial temperatures $\Delta T = T_\rho - T_z$, if they are close to each other. As the total energy of colliding particles should exceed $2\hbar\omega_0$ in order to enable the energy transfer, the rate of this process at temperatures $T < \hbar\omega_0$ becomes exponentially small: $\Delta\dot{E} \propto \Delta T \exp(-2\hbar\omega_0/T)$. Due to the presence of the energy gap $\hbar\omega_0$ in the excitation spectrum of the axial harmonic oscillator, the heat capacity of the axial degree of freedom is $dE_z/dT_z \sim \exp(-\hbar\omega_0/T)$, which leads to a thermalization rate $\Delta\dot{T}/\Delta T \propto \exp(-\hbar\omega_0/T)$. This exponential temperature dependence shows that the thermalization is suppressed at very low temperatures. One can cool the axial motion, but radially the cloud remains ''hot'' on a very long time scale.

II. 2D SCATTERING PROBLEM

First, we discuss the purely 2D elastic scattering in pair collisions of ultracold atoms interacting via a short-range potential $U(\rho)$. At interparticle distances $\rho \to \infty$ the wave function of colliding atoms is represented as a superposition of the incident plane wave and scattered circular wave [15],

$$\psi(\boldsymbol{\rho}) \approx e^{i\mathbf{q}\cdot\boldsymbol{\rho}} - f(q,\phi)\sqrt{\frac{i}{8\pi q\rho}}e^{iq\rho}. \tag{1}$$

The quantity $f(q,\phi)$ is the scattering amplitude, q is the relative momentum of the atoms, and ϕ the scattering angle. Note that $f(q,\phi)$ in Eq. (1) differs by a factor of $-\sqrt{8\pi q}$ from the 2D scattering amplitude defined in [15].

Similarly to the 3D case the scattering amplitude is governed by the contribution of the s-wave scattering if the relative momentum q satisfies the inequality $qR_e \ll 1$, where R_e is the characteristic radius of interaction. In the case of alkali atoms, the radius R_e is determined by the Van der Waals tail of the potential $U(\rho)$ and ranges from 20 Å for Li to 100 Å for Cs. The s-wave scattering amplitude is independent of the scattering angle ϕ. The probability $\alpha(q)$ for a scattered particle to pass through a circle of radius ρ per unit time is equal to the intensity of the scattered wave multiplied by $2\pi\rho v$, where $v = 2\hbar q/m$ is the relative velocity of colliding atoms. From Eq. (1) we have

$$\alpha(q) = \frac{\hbar}{2m}|f(q)|^2. \tag{2}$$

The velocity v is equal to the current density in the incident wave of Eq. (1). The ratio of $\alpha(q)$ to this quantity is the 2D cross section that has the dimension of length

$$\sigma(q) = |f(q)|^2/4q. \tag{3}$$

For the case of identical bosons, Eqs. (2) and (3) have an extra factor 2 in the right-hand side (rhs).

The quantity $\alpha(q)$ is nothing else than the rate constant of elastic collisions at a given q. The average of $\alpha(q)$ over the momentum distribution of atoms, multiplied by the number of pairs of atoms in a unit area, gives the number of scattering events in this area per unit time.

For finding the s-wave scattering amplitude one has to solve the Schrödinger equation for the s wave of the relative motion of colliding atoms at energy $\varepsilon = \hbar^2 q^2/m$

$$\left[-\frac{\hbar^2}{m}\Delta_\rho + U(\rho)\right]\psi_s(q,\rho) = \frac{\hbar^2 q^2}{m}\psi_s(q,\rho). \tag{4}$$

At distances $\rho \gg R_e$ the relative motion is free and one can omit the interaction between atoms. Then the solution of Eq. (4), which for $q\rho \gg 1$ gives the partial s wave of $\psi(\boldsymbol{\rho})$ Eq. (1), takes the form

$$\psi_s(q,\rho) = J_0(q\rho) - \frac{if(q)}{4}H_0(q\rho), \quad \rho \ll R_e, \tag{5}$$

where J_0 and H_0 are the Bessel and Hankel functions.

On the other hand, at distances $\rho \ll 1/q$ one can omit the relative energy of particles in Eq. (4). The resulting (zero energy) solution depends on the momentum q only through a normalization coefficient. In the interval of distances where $R_e \ll \rho \ll 1/q$, the motion is free and this solution becomes $\psi_s \propto \ln(\rho/d)$, where $d > 0$ is a characteristic length that depends on a detailed shape of the potential $U(\rho)$ and has to be found from the exact solution of Eq. (4) with $q = 0$. This logarithmic expression serves as a boundary condition for $\psi_s(q,\rho)$ Eq. (5) at $q\rho \ll 1$, which immediately leads to the scattering amplitude [15]

$$f(q) = \frac{2\pi}{\ln(1/qd_*) + i\pi/2}, \tag{6}$$

where $d_* = (d/2)\exp C$, and $C \approx 0.577$ is the Euler constant.

It is important to mention that the condition $qR_e \ll 1$ is sufficient for the validity of Eq. (6). This equation also holds for the case of resonance scattering, where the potential $U(\rho)$ supports a real (or virtual) weakly bound s level. In this case the spatial shape of $\psi_s(q,\rho)$ at distances where $R_e \ll \rho \ll 1/q$, is the same as the shape of the wave function of the weakly bound state. This gives $d_* = \hbar/\sqrt{m\varepsilon_0}$, where ε_0 is the binding energy. We thus have the inequality d_*

$\gg R_e$, and the quantity qd_* in Eq. (6) can be both small and large. The rate constant $\alpha(q)$ peaks at $q=1/d_*$ and decreases as $1/[1+(4/\pi^2)\ln^2(qd_*)]$ with increasing or decreasing q. Note that the 2D resonance is actually a resonance in the logarithmic scale of energies. The decrease of α by factor 2 from its maximum value requires a change of energy $\varepsilon=\hbar^2q^2/m$ by factor 20.

For $qd_*\ll 1$ one may omit the imaginary part in Eq. (6), and the scattering amplitude becomes real and positive [16,17]. The positive sign of $f(q)$ has a crucial consequence for the mean-field interparticle interaction in purely 2D Bose gases. In the ultracold limit, where $qR_e\ll 1$, the scattering amplitude is related to the energy of interaction in a pair of particles (coupling constant g). For a short-range potential $U(\rho)$, the energy of the mean-field interaction in a weakly interacting gas is the sum of all pair interactions. In a uniform Bose-condensed gas the coupling constant g for condensate atoms is equal to the amplitude of scattering (with an extra factor $\hbar^2/m$ for our definition of f) at the energy of the relative motion $\varepsilon=\hbar^2q^2/m=2\mu$, where μ is the chemical potential [18,19]. Hence, we have

$$g=\frac{\hbar^2}{m}f(q_c)=\frac{2\pi\hbar^2}{m}\frac{1}{\ln(1/q_cd_*)}>0, \quad q_cd_*\ll 1, \quad (7)$$

where $q_c=\sqrt{2m\mu}/\hbar$ is the inverse healing length. In a dilute thermal 2D gas, due to the logarithmic dependence of f on q, the thermal average of the mean-field interaction leads to the coupling constant $g=(\hbar^2/m)f(q_T)$, where $q_T=\sqrt{mT}/\hbar$ is the thermal momentum of particles. At sufficiently low temperatures, where $q_Td_*\ll 1$, we again have $g>0$.

Thus, in an ultracold purely 2D gas the coupling constant for the mean-field interaction is always positive in the dilute limit and, hence, the interaction is repulsive. This striking difference from the 3D case is a consequence of the 2D kinematics. For low energies, at interparticle distances $\rho\gg R_e$, the (free) relative motion of a pair of atoms is governed by the wave function $\psi_s\propto\ln(\rho/d)$. The probability density $|\psi_s|^2$ of finding two atoms at a given separation increases with ρ as the condition $\rho>d$ is always reached, unless the atoms have a bound state with energy $\varepsilon_0\to 0$ ($d\to\infty$). This means that it is favorable for particles to be at larger ρ, i.e., they repel each other.

III. SCATTERING IN AXIALLY CONFINED GEOMETRIES: GENERAL APPROACH

In this section we discuss elastic scattering of atoms (tightly) confined in the axial (z) direction, assuming that the motion in two other (x,y) directions is free. We analyze how the scattering is influenced by the confinement and calculate a complete set of scattering amplitudes corresponding to collision-induced transitions between particle states in the confining potential. We still call this scattering elastic as the internal states of atoms are not changing.

For a harmonic axial confinement, the motion of two atoms interacting with each other via the potential $V(r)$ can be still separated into their relative and center-of-mass motion. The latter drops out of the scattering problem. The relative motion is governed by the potential $V(r)$ and by the potential $V_H(z)=m\omega_0^2z^2/4$ originating from the axial confinement with frequency ω_0. For the incident wave characterized by the wave vector $\mathbf{q}$ of the motion in the (x,y) plane and by the quantum number ν of the state in the potential $V_H(z)$, the wave function of the relative motion satisfies the Schrödinger equation

$$\left[-\frac{\hbar^2}{m}\Delta+V(r)+V_H(z)-\frac{\hbar\omega_0}{2}\right]\psi(\mathbf{r})=\varepsilon\psi(\mathbf{r}), \quad (8)$$

where $\varepsilon=\hbar^2q^2/m+\nu\hbar\omega_0$.

The scattering depends crucially on the relation between the radius of interatomic interaction R_e and the characteristic de Broglie wavelength of particles $\tilde{\Lambda}_\varepsilon$. The latter is introduced qualitatively, as the motion along the z axis is tightly confined. Accounting for the zero point axial oscillations one can write $\tilde{\Lambda}_\varepsilon\sim\hbar/\sqrt{m\tilde{\varepsilon}}$, with $\tilde{\varepsilon}=\varepsilon+\hbar\omega_0/2$. We will consider the ultracold limit where

$$\tilde{\Lambda}_\varepsilon\gg R_e. \quad (9)$$

Equation (9) immediately leads to the inequality $qR_e\ll 1$, as the de Broglie wavelength for the motion in the (x,y) plane is $\sim 1/q$. For small ν the harmonic oscillator length $l_0=(\hbar/m\omega_0)^{1/2}$ plays the role of the axial de Broglie wavelength of atoms. Therefore, the ultra-cold limit (9) also requires the condition $l_0\gg R_e$. For large ν, the axial de Broglie wavelength is $\sim l_0/\sqrt{\nu}$ and, according to Eq. (9), this quantity should be much larger than R_e.

Under the condition $qR_e\ll 1$, the scattering amplitudes are determined by the contribution of the s wave for the motion in the (x,y) plane. In the case of identical bosons, the s-wave scattering requires even values of ν and ν' as the wave function ψ should conserve its sign under the transformation $z\to -z$. The quantum numbers ν and ν' should be even also for distinguishable particles. Otherwise at distances of interatomic interaction, $r\lesssim R_e$, the wave function ψ will be small at least as R_e/l_0, ensuring the presence of this small parameter in the expressions for the scattering amplitudes.

The scattering amplitudes corresponding to transitions from the initial state ν [of the relative motion in the potential $V_H(z)$] to final states ν' are defined through the asymptotic form of the wave function ψ at an infinite separation ρ in the (x,y) plane:

$$\psi(\mathbf{r})\approx\varphi_\nu(z)e^{i\mathbf{q}\cdot\boldsymbol{\rho}}-\sum_{\nu'}f_{\nu\nu'}(\varepsilon)\varphi_{\nu'}(z)\sqrt{\frac{i}{8\pi q_{\nu'}\rho}}e^{iq_{\nu'}\rho}, \quad (10)$$

where $\varphi_\nu(z)$ and $\varphi_{\nu'}(z)$ are the (real) eigenfunctions of the states ν and ν'. For each of the scattered circular waves the value of the momentum $q_{\nu'}$ follows from the energy-conservation law $\hbar^2q_{\nu'}^2/m=\varepsilon-\hbar\omega_0\nu'>0$.

Relying on the condition (9), we develop a method that allows us to express the scattering amplitudes through the 3D scattering length. At interparticle distances $r\gg R_e$ the relative motion in the (x,y) plane is free, and the motion along the z

axis is governed only by the harmonic oscillator potential $V_H(z)$. Then, the solution of Eq. (8) with $V(r)=0$ can be expressed through the Green function $G_\varepsilon(\mathbf{r},\mathbf{r}')$ of this equation. Retaining only the s wave for the motion in the (x,y) plane, we have

$$\psi(\mathbf{r})=\varphi_\nu(z)J_0(q\rho)+A_\nu G_\varepsilon(\mathbf{r},0), \tag{11}$$

and the expression for the Green function $G_\varepsilon(\mathbf{r},0)$ reads

$$G_\varepsilon(\mathbf{r},0)=\sum_{\nu'}\ \varphi_{\nu'}(z)\varphi_{\nu'}(0)\times\begin{cases} iH_0^{(1)}(q_{\nu'}\rho)/4, & q_{\nu'}^2>0 \\ K_0(|q_{\nu'}|\rho)/2\pi, & q_{\nu'}^2<0. \end{cases} \tag{12}$$

Here the summation is also performed over closed scattering channels for which $q_{\nu'}^2<0$. The function $K_0(x)=(i\pi/2)H_0(ix)$ and it decays as $\sqrt{\pi/2x}\exp(-x)$ at $x\gg 1$. Thus, for $\rho\to\infty$ the terms corresponding to the closed channels vanish. Then, comparing Eq. (11) at $\rho\to\infty$ with Eq. (10), we find a relation between the scattering amplitudes and the coefficients A_ν:

$$f_{\nu\nu'}=-A_\nu\varphi_{\nu'}(0)\,\theta(\varepsilon-\hbar\omega_0\nu'), \tag{13}$$

where θ is the step function.

The condition $l_0\gg R_e$ ensures that the relative motion of atoms in the region of interatomic interaction is not influenced by the axial (tight) confinement. Therefore, the wave function $\psi(\mathbf{r})$ in the interval of distances where $R_e\ll r\ll\tilde{\Lambda}_\varepsilon$, differs only by a normalization coefficient from the 3D wave function of free motion at zero energy. Writing this coefficient as $\eta\varphi_\nu(0)$, we have

$$\psi(r)\approx\eta\varphi_\nu(0)(1-a/r). \tag{14}$$

Equation (14) contains the 3D scattering length a and serves as a boundary condition for $\psi(\mathbf{r})$ Eq. (11) at $r\to 0$.

For $r\to 0$, a straightforward calculation of the sum in Eq. (12) yields

$$G_\varepsilon(r,0)\approx\frac{1}{4\pi r}+\frac{1}{2(2\pi)^{3/2}l_0}w\left(\frac{\varepsilon}{2\hbar\omega_0}\right), \tag{15}$$

where the complex function $w(x)$ is given by

$$w(x)=\lim_{N\to\infty}\left[2\sqrt{\frac{N}{\pi}}\ln\frac{N}{e^2}-\sum_{j=0}^{N}\frac{(2j-1)!!}{(2j)!!}\ln(j-x-i0)\right]. \tag{16}$$

With the Green function (15), the wave function (11) at $r\to 0$ should coincide with $\psi(r)$ Eq. (14). This gives the coefficient

$$\eta=\frac{1}{1+(a/\sqrt{2\pi}l_0)w(\varepsilon/2\hbar\omega_0)} \tag{17}$$

and provides us with the values of the coefficients A_ν. Then, using Eq. (13) and explicit expressions $\varphi_\nu(0)=(1/2\pi l_0^2)^{1/4}(\nu-1)!!/\sqrt{\nu!}$, we immediately obtain the scattering amplitude $f_{00}(\varepsilon)$ and express all other scattering amplitudes through this quantity:

$$f_{00}(\varepsilon)=4\pi\varphi_0^2(0)a\,\eta=\frac{2\sqrt{2\pi}}{l_0/a+(1/\sqrt{2\pi})w(\varepsilon/2\hbar\omega_0)}, \tag{18}$$

$$f_{\nu\nu'}(\varepsilon)=P_{\nu\nu'}f_{00}(\varepsilon)\,\theta(\varepsilon-\hbar\omega_0\nu)\,\theta(\varepsilon-\hbar\omega_0\nu'), \tag{19}$$

where

$$P_{\nu\nu'}=\frac{\varphi_\nu(0)\varphi_{\nu'}(0)}{\varphi_0^2(0)}=\frac{(\nu-1)!!(\nu'-1)!!}{\sqrt{\nu!\,\nu'!}}. \tag{20}$$

One can see from Eqs. (18) and (19) that the scattering amplitude is a universal function of the parameters a/l_0 and $\varepsilon/\hbar\omega_0$, irrespective of the values of ν and ν'. The quantity $P_{\nu\nu'}$ in Eq. (19) is nothing else than the relative probability amplitude of having an axial interparticle separation $|z|\ll l_0$ (in particular, $|z|\lesssim R_e$) for both incoming (ν) and outgoing (ν') channels of the scattering process. It is thus sufficient to study only the behavior of $f_{00}(\varepsilon)$.

We emphasize the presence of two distinct regimes of scattering. The first one, which we call quasi2D, requires relative energies $\varepsilon\ll\hbar\omega_0$. In this case, the relative motion of particles is confined to zero-point oscillations in the axial direction, and the 2D kinematics of the relative motion at interatomic distances $\rho>l_0$ should manifest itself in the dependence of the scattering amplitude on $\varepsilon/2\hbar\omega_0$ and a/l_0. In the other regime, at energies already comparable with $\hbar\omega_0$, the 2D kinematics is no longer pronounced in the scattering process. Nevertheless, the latter is still influenced by the (tight) axial confinement. Qualitatively, the scattering amplitudes become three dimensional, with a momentum $\sim 1/l_0$ related to the quantum character of the axial motion. Thus, we can say that this is a confinement-dominated 3D regime of scattering. With increasing the relative energy to $\varepsilon\gg\hbar\omega_0$, the momentum is increasing to $\sqrt{m\varepsilon}/\hbar$ and the confinement-dominated 3D regime continuously transforms to ordinary 3D scattering.

IV. QUASI-2D REGIME

In the quasi-2D regime, due to the condition $\varepsilon\ll\hbar\omega_0$, the incident and scattered waves have quantum numbers $\nu=\nu'=0$ for the motion in the axial harmonic potential $V_H(z)$. The relative energy $\varepsilon=\hbar^2q^2/m$ and the inequality $ql_0\ll 1$ is satisfied. In this case Eq. (16) gives

$$w(\varepsilon/2\hbar\omega_0)=\ln(B\hbar\omega_0/\pi\varepsilon)+i\pi, \tag{21}$$

where $B\approx 0.915$. Then our equation (18) recovers Eq. (11) of Ref. [9], obtained in this limit [20].

Using Eq. (21) we can represent $f_{00}(\varepsilon)$ Eq. (18) in the 2D form (6), with

$$d_*=(d/2)\exp C=\sqrt{\pi/B}\,l_0\exp(-\sqrt{\pi/2}\,l_0/a). \tag{22}$$

This fact has a physical explanation. Relying on the same arguments as in the purely 2D case, one finds that in the interval of distances where $l_0\ll\rho\ll 1/q$, the wave function $\psi\propto\varphi_0(z)\ln(\rho/d)$. On the other hand, for $\rho\gg l_0$ we have

$\psi(\mathbf{r})=\varphi_0(z)\psi_s(\rho)$, where ψ_s is given by the 2D expression (5) with $f(q)=f_{00}(\varepsilon)$. This follows from Eqs. (11)–(13), as all closed scattering channels ($\nu'\neq 0$) in Eq. (12) for the Green function $G_\varepsilon(\mathbf{r},0)$ have momenta $|q_{\nu'}|\gtrsim 1/l_0$ and will be exponentially suppressed at $\rho\gg l_0$. Matching the two expressions for the wave function ψ one immediately obtains the 2D equation (6). However, the parameter d_* in Eq. (22) can be found only from the solution of the quasi-2D scattering problem.

We thus conclude that the scattering problem in the quasi-2D regime is equivalent to the scattering in an effective purely 2D potential that leads to the same value of d_*. For positive $a\ll l_0$, this potential can be viewed as a (low) barrier, with a height $V_0\sim\hbar^2 a/m l_0^3$ and radius l_0. Hence, in the case of positive a we have a small (positive) scattering amplitude, in accordance with Eqs. (6) and (22). For a negative a satisfying the condition $|a|\ll l_0$, the effective potential is a shallow well that has a depth $|V_0|$ and radius l_0. This shallow well supports a weakly bound state with an exponentially small binding energy ε_0, which leads to an exponentially large d_* as follows from Eq. (22). As a result, we have a resonance energy dependence of the scattering amplitude f_{00} at a fixed ratio a/l_0, and a resonance behavior of f_{00} as a function of a/l_0 at a fixed $\varepsilon/\hbar\omega_0$.

The resonance in the energy dependence of f_{00} is quite similar to the logarithmic-scale resonance in the purely 2D case, discussed in Sec. II. The quasi-2D resonance is also described by Eq. (6), where the length d_* is now given by Eq. (22). As expected, the dependence of f_{00} on ε is smooth.

The resonance in the dependence of the quasi-2D scattering amplitude on a/l_0, appearing at $a<0$, has been found and discussed in [9]. Relying on the above-introduced effective 2D potential for the quasi-2D scattering, we can now explain this resonance on the same grounds as the resonance in the energy dependence of f_{00}. We will do this in terms of the relative energy ε and the binding energy in the effective potential, $\varepsilon_0=\hbar^2/md_*^2\propto\exp(-\sqrt{2\pi}l_0/|a|)$ $(a<0)$. For $\varepsilon/\varepsilon_0=(qd_*)^2\gg 1$, the scattering amplitude in Eq. (6) is real and negative. It increases in magnitude with decreasing ratio $\varepsilon/\varepsilon_0$, that is with decreasing q or l_0. In the opposite limit, where $\varepsilon/\varepsilon_0\ll 1$, the scattering amplitude is real and positive and it increases with the ratio $\varepsilon/\varepsilon_0$. The region of energies $\varepsilon/\varepsilon_0\sim 1$ corresponds to the resonance, where both the real and imaginary parts of f_{00} are important. The real part reaches its maximum at $\varepsilon/\varepsilon_0=\exp(-\pi)$, drops to zero at $\varepsilon/\varepsilon_0=1$, and acquires the maximum negative value for $\varepsilon/\varepsilon_0=\exp\pi$. The dependence of $\mathrm{Im}f_{00}$ on $\varepsilon/\varepsilon_0$ is the same as that of the quantity $|f_{00}|^2$. Both of them peak at $\varepsilon/\varepsilon_0=1$ and decrease with increasing or decreasing $\varepsilon/\varepsilon_0$.

Qualitatively, the picture remains the same for $|a|\sim l_0$. In Fig. 1 we present the dependence of $|f_{00}|^2$ on $\varepsilon/2\hbar\omega_0$ at a/l_0 equal to -1, 1, and ∞. In the two last cases we always have $\varepsilon/\varepsilon_0\ll 1$, and $|f_{00}|^2$ increases with ε at $\varepsilon\ll\hbar\omega_0$. For $a/l_0=-1$ we have the above-described logarithmic-scale resonance in the behavior of $|f_{00}|^2$.

The quasi-2D resonance is much more pronounced in the dependence of the scattering amplitude on the parameter a/l_0. The reason is that f_{00} logarithmically depends on the particle energy, whereas the dependence on a/l_0 is a power law. For $\varepsilon\ll\hbar\omega_0$, Eq. (18) yields

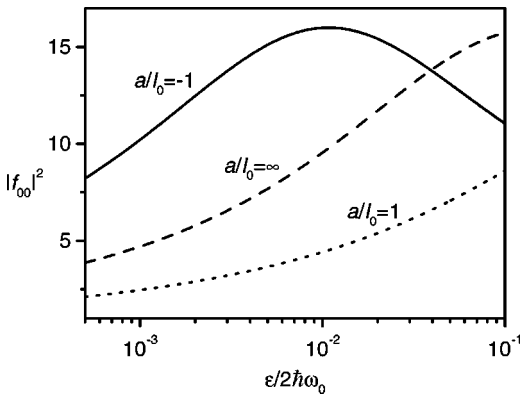

FIG. 1. The function $|f_{00}|^2$ versus the ratio $\varepsilon/2\hbar\omega_0$ for $a/l_0=-1$ (solid curve), $a/l_0=\infty$ (dashed curve) and $a/l_0=1$ (dotted curve).

$$|f_{00}|^2=\frac{16\pi^2}{(\sqrt{2\pi}\,l_0/a+\ln(B\hbar\omega_0/\pi\varepsilon))^2+\pi^2}. \qquad (23)$$

The quantity $|f_{00}|^2$ differs only by a factor of $\hbar/m$ from the rate constant of elastic collisions [see Eq. (2)], and one can think of observing the resonance dependence of $|f_{00}|^2$ on a/l_0 in an experiment. For example, one can keep ε (temperature) and ω_0 constant and vary a by using Feshbach resonances. The resonance is achieved at $a=-\sqrt{2\pi}l_0/\ln(B\hbar\omega_0/\pi\varepsilon)$. This is a striking difference from the 3D case, where the cross section and rate constant of elastic collisions monotonously increase with a^2.

In Fig. 2 we present $|f_{00}|^2$ versus a/l_0 at a fixed $\varepsilon/\hbar\omega_0$. In order to extend the results to the region of energies where the validity of the quasi-2D approach is questionable, the quantity $|f_{00}|^2$ was calculated by using Eq. (18) for the scattering amplitude. The resonance is still visible at $\varepsilon/\hbar\omega_0=0.06$ and it disappears for $\varepsilon/\hbar\omega_0=0.2$.

The obtained results allow us to conclude that for $|a|\gtrsim l_0$ the approximate border line between the quasi-2D and confinement-dominated 3D regimes is $\varepsilon\approx\varepsilon_*=0.1\hbar\omega_0$. For $|a|\ll l_0$, as we will see below, the confinement-dominated regime is practically absent.

The output of kinetic studies in thermal gases is usually related to the mean collisional frequency (the rate of interatomic collisions) $\Omega=\bar{\alpha}n$, where $\bar{\alpha}$ is the mean rate constant of elastic collisions, and n the gas density. In the quasi-2D regime, the rate constant $\bar{\alpha}$ follows directly from Eq. (2), with twice as large rhs for identical bosons,

$$\bar{\alpha}=\frac{\hbar}{m}\langle|f_{00}|^2\rangle, \qquad (24)$$

where the symbol $\langle\,\rangle$ stands for the thermal average. Our numerical calculations show that the average of $|f_{00}|^2$ over the Boltzmann distribution of particles only slightly broadens the resonances in Fig. 1 and Fig. 2. Due to the logarithmic dependence of f_{00} on the relative energy, the thermal average

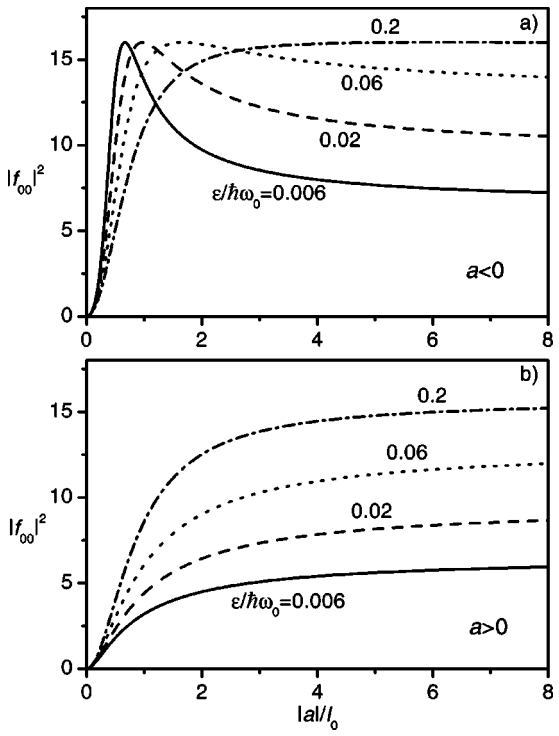

FIG. 2. The function $|f_{00}|^2$ versus $|a|/l_0$ at various ratios $\varepsilon/\hbar\omega_0$ for $a<0$ (a) and $a>0$ (b).

is obtained with a good accuracy if one simply replaces ε by the gas temperature T. Thus, in order to observe the manifestation of the 2D features of the particle motion in their collisional rates one has to achieve very low temperatures $T<0.1\hbar\omega_0$.

V. CONFINEMENT-DOMINATED 3D REGIME

In the confinement-dominated 3D regime, where $\varepsilon \sim \hbar\omega_0$, the axial confinement influences the scattering process through the confined character of the axial motion. In order to analyze this influence, we first examine the function $w(\varepsilon/2\hbar\omega_0)$ that determines the energy dependence of the scattering amplitudes. The imaginary part of $w(x)$, following from Eq. (16), is equal to

$$\mathrm{Im}w(x)=\pi\sum_{j=0}^{[x]}\frac{(2j-1)!!}{(2j)!!}=2\sqrt{\pi}\,\frac{\Gamma([x]+3/2)}{[x]!}, \quad (25)$$

where $[x]$ is the integer part of x. The function $\mathrm{Im}w(x)$ has a stepwise behavior as shown in Fig. 3. It is constant at noninteger x and undergoes a jump at each integer x, taking a larger value for larger x. With increasing x, the jumps become smaller and for $x\gg 1$ we have $\mathrm{Im}w(x)\approx 2\sqrt{\pi x}$. The real part of $w(x)$ was calculated numerically from Eq. (16) and is also given in Fig. 3. At any x we have $|\mathrm{Re}w(x)|<1$, except for narrow intervals in the vicinity of integer x. In each of these intervals the function $\mathrm{Re}w(x)$ logarithmically goes to infinity as x approaches the corresponding integer value. This is consistent with the stepwise behavior of

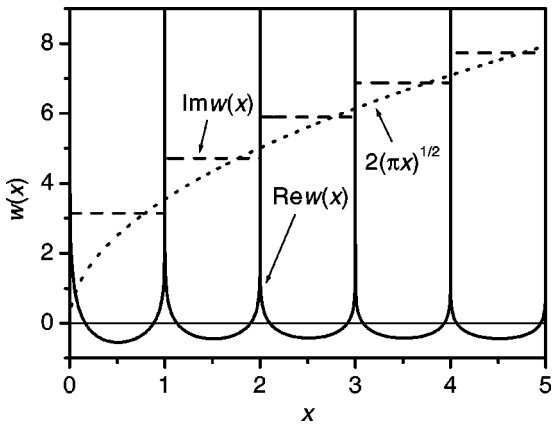

FIG. 3. The functions $\mathrm{Re}w(x)$ (solid curve) and $\mathrm{Im}w(x)$ (dashed lines). The dotted curve shows the function $2\sqrt{\pi x}$ corresponding to the asymptotic behavior of Imw at large x.

$\mathrm{Im}w(x)$: As one can see directly from Eq. (16), for x approaching an integer j the analytical complex function $w \propto \ln(j-x-i0)$.

The described behavior of the function $w(\varepsilon/2\hbar\omega_0)$ has a direct influence on the scattering amplitudes. For $\varepsilon/2\hbar\omega_0$ close to an integer j, the amplitude is small and it is equal to zero for $\varepsilon=2\hbar\omega_0 j$. This phenomenon originates from the fact that for ε close to $2\hbar\omega_0 j$, a new scattering channel opens (really or virtually). For this channel the momentum $|q_{\nu'}|=\sqrt{m|\varepsilon-2\hbar\omega_0 j|}/\hbar$ is very small. Hence, at distances $\rho\ll|1/q_{\nu'}|$ the wave function ψ [Eq. (11)] will be determined by the contribution of this low-momentum term if $\rho\gg l_0$. This is clearly seen from Eqs. (12) and (11) and makes the situation somewhat similar to that in the quasi-2D regime of scattering. In the latter case, the wave function ψ in Eq. (11) at distances $\rho\ll 1/q$ is also determined by the contribution of the low-momentum channel as long as $\rho\gg l_0$. Then, as follows from the analysis in Sec. IV, this wave function and the scattering amplitude f_{00} behave as $1/\ln(\hbar\omega_0/\varepsilon)$ in the limit $\varepsilon\to 0$. In the present case, the wave function ψ and the scattering amplitudes are small as $1/\ln(\hbar\omega_0/|\varepsilon-2\hbar\omega_0 j|)$ for $\varepsilon\to 2\hbar\omega_0 j$.

The dependence of $|f_{00}|^2$ on $\varepsilon/2\hbar\omega_0$ for a/l_0 equal to -1, 1, and ∞ is displayed in Fig. 4. Outside narrow energy intervals in the vicinity of integer $\varepsilon/2\hbar\omega_0$, the quantity $|f_{00}|^2$ is a smooth function of ε. One can also see a sort of a stepwise decrease of $|f_{00}|^2$ with increasing ε, originating from the stepwise increase of the function $\mathrm{Im}w(\varepsilon/2\hbar\omega_0)$. For $\varepsilon/2\hbar\omega_0$ close to integer values $j>0$ we find a fine structure similar in nature to the behavior of $|f_{00}|^2$ at $\varepsilon\ll\hbar\omega_0$. For $a/l_0=1$ and $a/l_0=\infty$ there are narrow dips corresponding to the logarithmic decrease of $|f_{00}|^2$ as $\varepsilon\to 2\hbar\omega_0 j$, and for $a/l_0=-1$ these dips are accompanied by resonances. Note that the thermal distribution of particles averages out this fine structure, and the latter will not be pronounced in kinetic properties.

The difference between the confinement-dominated 3D regime and the ordinary 3D regime of scattering will manifest itself in the rate of elastic collisions (mean collisional frequency Ω). For the Boltzmann distribution of particles,

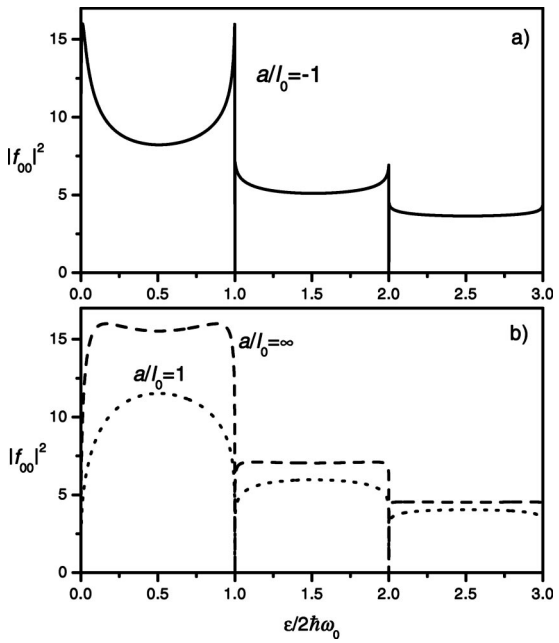

FIG. 4. The function $|f_{00}|^2$ versus the ratio $\varepsilon/2\hbar\omega_0$. In (a) the parameter $a/l_0=-1$. In (b) the dashed curve corresponds to the unitarity limit ($a/l_0=\infty$), and the dotted curve to $a/l_0=1$.

one can find this quantity by turning to the thermal distribution for the relative motion of colliding partners. Collision-induced transitions between the states of the relative motion in the axial potential $V_H(z)$ are described by the rate constants

$$\alpha_{\nu\nu'}(\varepsilon)=(\hbar/m)|f_{\nu\nu'}(\varepsilon)|^2, \tag{26}$$

where the scattering amplitudes $f_{\nu\nu'}$ are given by Eqs. (18) and (19), and an extra factor 2 for identical bosons is taken into account. The collisional frequency $\Omega=\overline{\alpha}n$, where n is the (2D) density, and the mean rate constant of elastic collisions, $\overline{\alpha}$, is obtained by averaging $\alpha_{\nu\nu'}$ in Eq. (26) over the thermal distribution of relative energies ε and by making the summation over all possible scattering channels. We thus have

$$\Omega=\overline{\alpha}n=\sum_{\nu\nu'}\int\frac{n\Lambda_T^2 d^2q}{(2\pi)^2}\alpha_{\nu\nu'}(\varepsilon)A\exp\left(-\frac{\varepsilon}{T}\right). \tag{27}$$

Here $\Lambda_T=(2\pi\hbar^2/mT)^{1/2}$ is the thermal de Broglie wavelength $\varepsilon=\hbar^2q^2/m+\hbar\omega_0\nu$ and the quantum numbers ν and ν' take only even values. The distribution function over ν and q is normalized to unity. The normalization coefficient A is obtained by the summation over both even and odd ν and is equal to

$$A=2[1-\exp(-\hbar\omega_0/T)]. \tag{28}$$

Note that the number of collisions per unit time and unit surface area in the (x,y) plane is equal to $\overline{\alpha}n^2/2=\Omega n/2$.

The manifestation of the tight axial confinement of the particle motion in collisional rates depends on the relation between the scattering length a and the characteristic de Broglie wavelength $\tilde{\Lambda}_\varepsilon\sim\hbar/\sqrt{m(\varepsilon+\hbar\omega_0/2)}$ accounting for the zero-point axial oscillations. For the scattering length satisfying the condition $|a|\ll\tilde{\Lambda}_\varepsilon$, the scattering amplitudes are energy independent at any ε, except for extremely small energies in the quasi-2D regime. This follows directly from Eqs. (17)–(19). The condition $|a|\ll\tilde{\Lambda}_\varepsilon$ automatically leads to the inequalities $|a|\ll l_0$ and $|a|\ll\hbar/\sqrt{m\varepsilon}$. Hence, the function $w(\varepsilon/2\hbar\omega_0)$ is much smaller than $l_0/|a|$, unless $\varepsilon\lesssim\hbar\omega_0\exp(-l_0/|a|)$ [see Eq. (21) and Fig. 3]. Accordingly, Eq. (17) gives $\eta=1$ and Eqs. (18) and (19) lead to the scattering amplitudes

$$f_{\nu\nu'}=4\pi a\varphi_\nu(0)\varphi_{\nu'}(0)\theta(\varepsilon-\hbar\omega_0\nu)\theta(\varepsilon-\hbar\omega_0\nu'). \tag{29}$$

The amplitudes (29) are nothing else than the 3D scattering amplitude averaged over the axial distribution of particles in the incoming (ν) and outgoing (ν') scattering channels. From Eqs. (26) and (29) one obtains the same rate of transitions $\nu\to\nu'$ as in the case of 3D scattering of particles harmonically confined in the axial direction and interacting with each other via the potential $V(r)$. This is what one should expect, since under the condition $|a|\ll\tilde{\Lambda}_\varepsilon$ the amplitude of 3D scattering is momentum independent. The integration over d^2q in Eq. (27) leads to the mean collisional frequency

$$\Omega=\frac{\hbar n}{2m}(4\pi a)^2A\sum_{\nu,\nu'}\varphi_\nu^2(0)\varphi_{\nu'}^2(0)\exp\left(-\frac{\hbar\omega_0}{T}\max\{\nu,\nu'\}\right).$$

Thus, in the case where $|a|\ll\tilde{\Lambda}_T$, the tight confinement in the axial direction can manifest itself in the collisional rates only through the axial distribution of particles and the discrete structure of quantum levels in the axial confining potential. The expression for the collisional frequency Ω can be reduced to the form

$$\Omega=\frac{8\pi\hbar n}{m}\left(\frac{a}{l_0}\right)^2\xi, \tag{30}$$

where the coefficient ξ ranges from 1 at $T\ll\hbar\omega_0$ to $2/\pi$ for $T\gg\hbar\omega_0$. The condition $|a|\ll\tilde{\Lambda}_T$ is equivalent to $|a|\ll l_0$ and $q_T|a|\ll1$, where $q_T=\sqrt{mT}/\hbar$ is the thermal momentum of particles. For $T\gg\hbar\omega_0$, Eq. (30) gives the collisional frequency that coincides with the three-dimensional result averaged over the classical Boltzmann profile of the 3D density in the axial direction $n_B(z)$,

$$\Omega_{3D}=\langle\sigma_{3D}v\rangle\int\frac{n_B^2(z)}{n}dz. \tag{31}$$

Here σ is the 3D elastic cross section, and v is the relative velocity of colliding particles. In other words, the quantity $(1/2)\overline{\alpha}n^2=(1/2)\Omega n$ coincides with the number of 3D collisions per unit time and unit surface area in the (x,y) plane, given by $(1/2)\langle\sigma_{3D}v\rangle\int n_B^2(z)dz$.

From Eq. (30) we conclude that for $|a|\ll l_0$ the confinement-dominated 3D regime of scattering is not pronounced. At temperatures $T\lesssim\hbar\omega_0$ the collisional rate only slightly deviates from the ordinary 3D behavior. This has a

simple physical explanation. For $|a| \ll \tilde{\Lambda}_T$, treating collisions as three dimensional we have $\Omega \sim 8\pi a^2 v n_{3D}$. At low temperatures $T \lesssim \hbar\omega_0$ the velocity $v \sim \hbar/m l_0$, and the 3D density is $n_{3D} \sim n/l_0$. For $T \gg \hbar\omega_0$ we have $v \sim (T/m)^{1/2}$ and $n_{3D} \sim n(m\omega_0^2/T)^{1/2}$. In both cases the ''flux'' $v n_{3D} \sim \omega_0 n$, and there is only a small numerical difference between the low-T and high-T collisional frequencies.

The ultracold limit (9) assumes that the characteristic radius of interatomic interaction $R_e \ll l_0$. Therefore, the condition $|a| \ll l_0$ is always satisfied, unless the scattering length is anomalously large ($|a| \gg R_e$). Below we will focus our attention on this case, assuming that $|a| \gtrsim l_0$.

Let us first show how the 3D result follows from our analysis at $T \gg \hbar\omega_0$, irrespective of the relation between a and $\tilde{\Lambda}_\varepsilon$. At these temperatures the main contribution to the sum in Eq. (27) comes from $\varepsilon \gg \hbar\omega_0$ and large ν and ν'. Accordingly, we can replace the summation over ν and ν' by integration. At energies much larger than $\hbar\omega_0$ the quantity $\sqrt{\nu}/l_0$ is nothing else than the axial momentum k_z and we have $\varepsilon = \hbar^2(q^2 + k_z^2)/m$. For these energies the function $w(\varepsilon/2\hbar\omega_0)$ in Eq. (18) takes its asymptotic form $w \approx i\sqrt{2\pi\varepsilon/\hbar\omega_0}$. Using Eq. (19), this immediately allows us to write

$$|f_{\nu\nu'}|^2 = P_{\nu\nu'}^2 \frac{8\pi a^2}{l_0^2(1+p^2a^2)} = P_{\nu\nu'}^2 \frac{\sigma_{3D}}{l_0^2}, \quad \nu' < \frac{\varepsilon}{\hbar\omega_0},$$

where $p = \sqrt{q^2 + k_z^2}$ is the 3D momentum of the relative motion, and $\sigma_{3D} = 8\pi a^2/(1+p^2a^2)$ is the cross section for the 3D elastic scattering. For large ν and ν', Eq. (20) gives $P_{\nu\nu'} = (4/\pi^2\nu\nu')^{1/4}$, and the integration over ν' in Eq. (27) multiplies σ_{3D} by the relative 3D velocity v. Then, turning from the integration over ν to the integration over the axial momentum, we reduce Eq. (27) to

$$\Omega = \int \frac{n\Lambda_T^2 d^3p}{(2\pi)^3} (\sigma_{3D} v) A \exp\left(-\frac{\hbar^2 p^2}{mT}\right), \tag{32}$$

and one can easily check that Eq. (32) coincides with the three-dimensional result Ω_{3D} in Eq. (31).

In the limiting case, where the thermal momentum of particles satisfies the inequality $q_T|a| \gg 1$, we obtain

$$\Omega_{3D} = \frac{16\hbar n}{m}\left(\frac{\hbar\omega_0}{T}\right), \quad q_T|a| \gg 1. \tag{33}$$

In the opposite limit, where $q_T|a| \ll 1$, at temperatures $T \gg \hbar\omega_0$ we automatically have $|a| \ll \Lambda_T$ and, accordingly, recover Eq. (30) with $\xi = 2/\pi$:

$$\Omega_{3D} = \frac{16\hbar n}{m}\left(\frac{a}{l_0}\right)^2, \quad q_T|a| \ll 1. \tag{34}$$

As mentioned in Sec. IV, for $|a| \gtrsim l_0$ the approximate border line between the quasi2D and confinement-dominated 3D regimes is $\varepsilon_* \approx 0.1\hbar\omega_0$. In the temperature interval $\varepsilon_* < T < \hbar\omega_0$, the leading scattering channel will be the same as in the quasi-2D case, that is $\nu = \nu' = 0$. However, the expression for the scattering amplitude f_{00} is different. From Fig. 3 and Eq. (18) one concludes that the real part of the function w can be neglected and the scattering amplitude takes the form

$$f_{00} = \frac{2\sqrt{2\pi}}{l_0/a + i\sqrt{\pi/2}}.$$

Then, retaining only the scattering channel $\nu = \nu' = 0$, Eqs. (26) and (27) yield

$$\Omega = \frac{8\pi\hbar n}{m}\left(\frac{a}{l_0}\right)^2 \frac{1 - \exp(-\hbar\omega_0/T)}{1 + \pi a^2/2l_0^2}. \tag{35}$$

The difference of Eq. (35) from the quasi-2D result of Eqs. (23) and (24) is related to the absence of the logarithmic term in the denominator. This follows from the fact that now we omitted the real part of the function w, which is logarithmically large in the quasi-2D regime.

It is worth noting that for $l_0 \gg |a|$, Eq. (35) is only slightly different from the 3D result (34). This is consistent with the above-given analysis leading to Eq. (30).

On the other hand, for large $|a|/l_0$ the difference between Eq. (35) and the 3D result (33) is significant. This originates from the fact that for a large scattering length a the 3D amplitude of scattering in the ultracold limit depends on the particle momenta. For a tight axial confinement, treating collisions as three dimensional, the relative momentum of colliding particles at temperatures $T \lesssim \hbar\omega_0$ is $\sim 1/l_0$ and it no longer depends on temperature. Hence, the scattering rate is quite different from that in 3D. Given these arguments, one expects a strongly pronounced confinement-dominated 3D regime of scattering if the ratio $|a|/l_0 \gg 1$.

This is confirmed by our numerical calculations for the temperature dependence of Ω from Eq. (27). In Fig. 5 we present the results for a/l_0 equal to -1, 1, and ∞. The largest deviation from the 3D regime is observed in the unitarity limit ($a \to \infty$). From Fig. 5 we see that in the Stanford [6] and ENS [8] experiments performed in this limit [21,22] one should have significant deviations of collisional rates from the ordinary 3D behavior.

VI. THERMALIZATION RATES

We will now discuss the collision-induced energy exchange between axial and radial degrees of freedom of the particle motion in an ultracold Bose gas tightly confined in the axial direction of a pancake-shaped trap. It is assumed that the radial confinement is shallow and it does not influence the scattering amplitudes. In this geometry, using degenerate Raman sideband cooling, the Stanford [5,6] and ENS [7,8] groups created Cs gas clouds with different axial (T_z) and radial (T_ρ) temperatures. After switching off the cooling, interatomic collisions lead to energy exchange between the axial and radial particle motion and the temperatures T_z and T_ρ start to approach each other. Ultimately, the gas reaches a new equilibrium state, with a temperature in between the initial T_z and T_ρ. The corresponding (thermalization) rate has been measured at Stanford [6] and ENS [8]

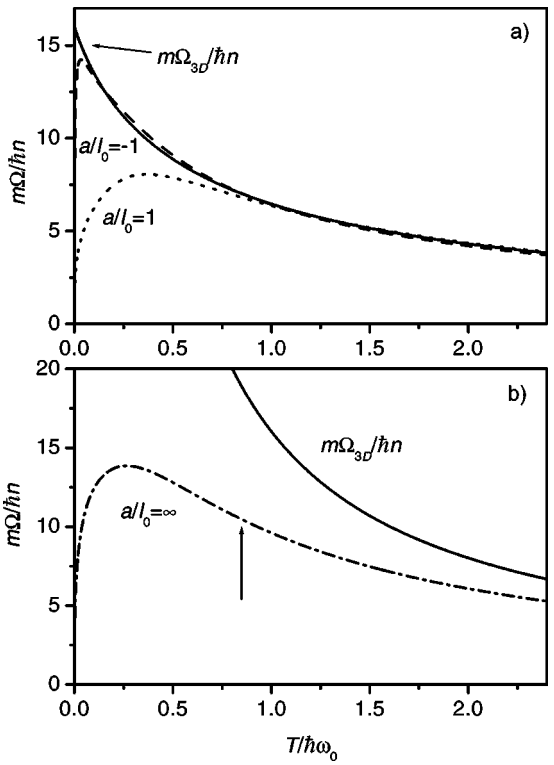

FIG. 5. The dimensionless quantity $m\Omega/\hbar n$ versus the ratio $T/\hbar\omega_0$. In (a) the parameter $a/l_0=-1$ (dashed curve), and $a/l_0=1$ (dotted curve). In (b) $a/l_0=\infty$ (unitarity limit). The solid curves in (a) and (b) show the 3D result (31). The arrow in (b) indicates the lowest ratio $T/\hbar\omega_0$ in the Stanford and ENS experiments.

and it provides us with the information on the regimes of interatomic collisions in the gas.

The radial motion of particles is classical. Therefore, we will calculate the rate of energy exchange between the radial and axial degrees of freedom for a given value of the radial coordinate $\boldsymbol{\rho}$ and then average the result over the Boltzmann density profile in the radial direction. The latter is given by

$$n(\rho)=n(0)\exp\left(-\frac{m\omega^2\rho^2}{2T}\right), \tag{36}$$

where $n(0)=m\omega^2N/2\pi T$ is the 2D density for $\rho=0$, ω the radial frequency, and N the total number of particles. Collision-induced transitions $\nu\rightarrow\nu'$ change the energy of the axial motion by $\hbar\omega_0(\nu'-\nu)$. We will assume that in the course of evolution the axial and radial distribution of particles remain Boltzmann, with instantaneous values of T_z and T_ρ. Then the rate of energy transfer from the radial to axial motion can be written on the same grounds as Eq. (27) and reads

$$\dot{E}_z=-\dot{E}_\rho=\frac{1}{2}\int n^2(\rho)d^2\rho\sum_{\nu\nu'}\int\frac{\Lambda_T^2d^2q}{(2\pi)^2}\hbar\omega_0(\nu'-\nu)\times\frac{\hbar}{m}|f_{\nu\nu'}(\varepsilon)|^2A\exp\left(-\frac{\hbar^2q^2}{mT_\rho}-\frac{\hbar\omega_0\nu}{T_z}\right), \tag{37}$$

where $\varepsilon=\hbar^2q^2/m+\hbar\omega_0\nu$, and the normalization coefficient A depends now on both T_z and T_ρ.

The radial energy of the gas is $E_\rho=2NT_\rho$, and the axial energy is given by $E_z=N\hbar\omega_0[\exp(\hbar\omega_0/T_z)-1]^{-1}$. The time derivatives of these energies take the form

$$\dot{E}_z=\frac{N\hbar^2\omega_0^2\dot{T}_z}{4T_z^2\sinh^2(\omega_0/2T_z)},\quad \dot{E}_\rho=2N\dot{T}_\rho. \tag{38}$$

Given the initial values of T_z and T_ρ, Eqs. (37) and (38) provide us with the necessary information on the evolution of $T_z(t)$ and $T_x(t)$.

For a small difference $\delta T=T_\rho-T_z$, these equations can be linearized with respect to δT. As the total energy is conserved, Eqs. (38) reduce to

$$\dot{\delta T}=\frac{\dot{E}_z}{N}\left(\frac{1}{2}+\frac{4T^2\sinh^2(\hbar\omega_0/2T)}{\hbar^2\omega_0^2}\right). \tag{39}$$

In Eq. (37) we represent the exponent as $-(\varepsilon/T+\delta T\hbar\omega_0\nu/T^2)$ and turn from the integration over dq to integration over $d\varepsilon$. The zero-order term of the expansion in powers of δT vanishes. The (leading) linear term, being substituted into Eq. (39), leads to the differential equation for $\delta T(t)$:

$$\dot{\delta T}=-\Omega_{th}(T)\,\delta T, \tag{40}$$

where the thermalization rate $\Omega_{th}(T)$ is given by

$$\Omega_{th}=\frac{n(0)\Lambda_T^2A}{16\pi\hbar}\left(\frac{\hbar^2\omega_0^2}{2T^2}+4\sinh^2(\hbar\omega_0/2T)\right)\times\sum_{\nu>\nu'}(\nu-\nu')^2\int_{\hbar\omega_0\nu}^{\infty}d\varepsilon|f_{\nu\nu'}(\varepsilon)|^2\exp\left(-\frac{\varepsilon}{T}\right). \tag{41}$$

The degeneracy parameter is $n(0)\Lambda_T^2=N(\hbar\omega/T)^2$ and it is small as the gas obeys the Boltzmann statistics. The normalization coefficient A is again given by Eq. (28).

The quantum numbers ν and ν' take only even values and, hence, in order to change the state of the axial motion one should have a relative energy $\varepsilon>2\hbar\omega_0$. Therefore, at temperatures lower than $\hbar\omega_0$ the rate of transitions changing the axial and radial energy is $\propto\exp(-2\hbar\omega_0/T)$. On the other hand, the axial energy $E_z\propto\exp(-\hbar\omega_0/T)$ and thus the thermalization rate $\Omega_{th}\propto\exp(-\hbar\omega_0/T)$. This can be easily found from Eq. (41) and shows that the quantum character of the axially confined particle motion exponentially suppresses the thermalization process at temperatures $T\ll\hbar\omega_0$. In particular, this is the case for the quasi-2D regime.

In the most interesting part of the confinement-dominated 3D regime, where $\varepsilon_*<T<\hbar\omega_0$, the energy exchange between the axial and radial motion of particles is mostly related to transitions between the states with $\nu'=0$ and $\nu=2$. The relative energy ε should be larger than $2\hbar\omega_0$ and, at the same time, this energy is well below $4\hbar\omega_0$. Hence, the scat-

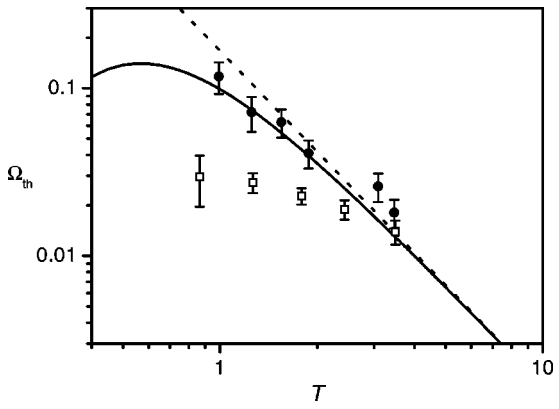

FIG. 6. Thermalization rate Ω_{th} (in units of Ω_0) versus temperature (in units of $\hbar\omega_0$) in the unitarity limit ($a=\infty$). The solid curve shows the result of our calculations for Ω_{th}, and the dotted line the 3D result Ω_{th}^{3D}. Squares and circles show the data of the Stanford and ENS experiments.

tering amplitude $f_{20}(\varepsilon)$ is determined by Eqs. (18) and (19) in which one can put $w(\varepsilon/2\hbar\omega_0)\approx i3\pi/2$ (see Eq. (25) and Fig. 3). This gives

$$f_{20}=\frac{2\sqrt{2\pi}}{l_0/a+i(3/2)\sqrt{\pi/2}},$$

and from Eq. (41) we obtain

$$\Omega_{th}=\frac{16\hbar\omega_0}{9\pi T}\Omega_0\frac{\exp(-\hbar\omega_0/T)}{1+8l_0^2/9\pi a^2}[1-\exp(-\hbar\omega_0/T)]^3. \tag{42}$$

The characteristic frequency Ω_0 is given by

$$\Omega_0=\omega^2N/\omega_0. \tag{43}$$

At temperatures $T\gg\hbar\omega_0$, Eq. (41) leads to the 3D result for the thermalization rate:

$$\Omega_{th}^{3D}=\frac{8}{15\pi}\left(\frac{\hbar\omega_0}{T}\right)^2\Omega_0, \quad q_T|a|\gg 1, \tag{44}$$

$$\Omega_{th}^{3D}=\frac{16}{15\pi}\left(\frac{a}{l_0}\right)^2\left(\frac{\hbar\omega_0}{T}\right)\Omega_0, \quad q_T|a|\ll 1. \tag{45}$$

Comparing Eqs. (44) and (45) with Eq. (42) one sees that Ω_{th} should acquire its maximum value at $T\sim\hbar\omega_0$. For $|a|\gtrsim l_0$ this maximum value is on the order of $\Omega_0/2\pi$.

As one expects from the discussion in Sec. V, the difference of the thermalization rate from Ω_{th}^{3D} is pronounced for large values of a. For example, in the unitarity limit Eq. (44) gives $\Omega_{th}^{3D}\propto 1/T^2$, whereas in the confinement-dominated regime we have $\Omega_{th}\propto(1/T)\exp(-\hbar\omega_0/T)$.

It should be emphasized that for any T, ω_0, and a the ratio Ω_{th}/Ω_0 depends only on the parameters $T/\hbar\omega_0$ and a/l_0. This can be found directly from Eq. (41). In Fig. 6 we present the temperature dependence of Ω_{th} in the unitarity limit, obtained numerically from Eq. (41), and compare our results with the data of the Stanford [6] and ENS [8] experiments. With the current error bars, the ENS results do not show significant deviations from the classical 3D behavior. These results agree fairly well with our calculations. The Stanford experiment gives somewhat lower values of Ω_{th}/Ω_0 at the lowest temperatures of the experiment.

In the hydrodynamic regime for the gas cloud, where the characteristic collisional frequency greatly exceeds the radial frequency ω, our assumption of quasiequilibrium at instantaneous (time-dependent) values of T_z and T_ρ may not be valid. Nevertheless, the shape of the curve $\Omega_{th}(T)$ qualitatively remains the same, including the exponential decrease with temperature at $T<\hbar\omega_0$ and power-law decrease with increasing T at temperatures larger than $\hbar\omega_0$. However, the maximum value of Ω_{th} will be somewhat lower (in particular, of the order of ω [6]).

The number of particles (per ''2D'' sheet of atoms) in the Stanford experiment [6] was $N\sim 10^4$ [23], which is by a factor of 20 higher than at ENS for $T\approx\hbar\omega_0$ [8]. We then estimate the 2D density of atoms for these temperatures to be $n\sim 2.5\times 10^8$ cm^{-2} at Stanford ($\omega\approx 90$ Hz), and $n\sim 0.5\times 10^8$ cm^{-2} at ENS ($\omega\approx 180$ Hz). For these densities, the ratio of the collisional frequency Ω in Fig. 5 to the radial frequency is $\Omega/\omega\sim 0.3$ in the ENS experiment, and $\Omega/\omega\sim 3$ in the experiment at Stanford. At temperatures $T>\hbar\omega_0$ the density n and the ratio Ω/ω are smaller in both experiments. We thus see that the ENS experiment [8] was in the collisionless regime, although rather close to the hydrodynamic regime at temperatures $T\approx\hbar\omega_0$. For these temperatures, the Stanford experiment [6] has already achieved the hydrodynamic regime, and this can explain the discrepancy between our calculations and the Stanford results in Fig. 6.

VII. INELASTIC TWO-BODY PROCESSES

Inelastic scattering of atoms is also influenced by the tight axial confinement of the particle motion. In this section we will consider the inelastic two-body processes, such as spin relaxation, in which the internal states of colliding atoms are changing, and the released internal-state energy of the atoms is transferred to their kinetic energy. Our goal is to establish a relation between the inelastic rates in 3D and those in the (tightly) axially confined geometry. The analysis given below relies on two important conditions widely met for the two-body spin relaxation [24].

(i) The energy release per collision greatly exceeds the gas temperature and the frequency of the axial confinement. Accordingly, the inelastic transitions occur at comparatively short interparticle distances $\sim R_{in}$ that are much smaller than the characteristic de Broglie wavelength of particles.

(ii) The inelastic transitions are caused by weak (spin-dipole, spin-orbit, etc.) interatomic interactions and can be treated with perturbation theory.

To first order in perturbation theory the amplitude of inelastic scattering, defined in the same way as in the previous sections, is given by a general expression [25]

$$f_{in}(\varepsilon)=\frac{m}{\hbar^2}\int \psi_i(\mathbf{r})U_{int}(\mathbf{r})\psi_f(\mathbf{r})d^3r. \tag{46}$$

Here $\psi_i(\mathbf{r})$ and $\psi_f(\mathbf{r})$ are the true wave functions of the initial and final states of the relative motion of colliding atoms, and $U_{int}(\mathbf{r})$ is the (weak) interatomic potential responsible for inelastic transitions. This potential is the same as in the 3D case. The function ψ_f is also the same as in 3D, since the relative energy in the final state is much larger than $\hbar\omega_0$. Thus, the only difference of the amplitude f_{in} in Eq. (46) from the amplitude of inelastic scattering in the 3D case is related to the form of the wave function ψ_i.

The characteristic interatomic distance R_{in} at which the inelastic transitions occur, satisfies the inequality $R_{in} \ll \tilde{\Lambda}_\varepsilon$ [see item (i)]. Therefore, we are in the ultracold limit similar to that determined by Eq. (9) in the case of elastic scattering, and the conditions $qR_{in} \ll 1$ and $R_{in} \ll l_0$ are satisfied. The former ensures a dominant contribution of the *s* wave (of the initial wave function ψ_i) to the scattering amplitude f_{in} in Eq. (46). Due to the condition $R_{in} \ll l_0$, at distances $r \sim R_{in}$ the wave function ψ_i has a three-dimensional character: $\psi_i(r) \propto \tilde{\psi}_{3D}(r)$, where $\tilde{\psi}_{3D}(r)$ is the wave function of the 3D relative motion at zero energy. For $r \gg R_e$ we have $\tilde{\psi}_{3D}(r) = (1 - a/r)$, and in order to be consistent with Eq. (14) we should write

$$\psi_i(r) = \eta(\varepsilon)\varphi_\nu(0)\tilde{\psi}_{3D}(r), \tag{47}$$

where the coefficient $\eta(\varepsilon)$ is given by Eq. (17), and ν is the quantum number of the initial state of the relative motion in the axial harmonic potential $V_H(z)$.

In the 3D case, the amplitude f_0 of inelastic scattering at zero initial energy is determined by Eq. (46) with ψ_i replaced by $\tilde{\psi}_{3D}$. Hence, Eq. (47) directly gives a relation between the two scattering amplitudes

$$f_{in} = \eta(\varepsilon)\varphi_\nu(0) f_0. \tag{48}$$

Due to the high relative kinetic energy of particles in the final state of the inelastic channel, the density of final states in this channel is independent of the axial confinement. Therefore, relying on Eq. (48) the mean rate constant $\bar{\alpha}_{in}$ of inelastic collisions in the axially confined geometry and the corresponding collisional frequency Ω_{in} can be represented in the form

$$\bar{\alpha}_{in} = \langle |\eta(\varepsilon)|^2 \varphi_\nu^2(0)\, \theta(\varepsilon - \hbar\omega_0\nu)\rangle \alpha_0, \quad \Omega_{in} = \bar{\alpha}_{in} n, \tag{49}$$

where α_0 is the 3D inelastic rate constant at zero energy.

Note that in the ultracold limit the 3D inelastic rate constant is temperature independent and equal to α_0 if the scattering length $|a| \lesssim R_e$. For $|a| \gg R_e$, the wave function of the relative motion in the region of interatomic interaction takes the form $\psi_i(r) = \eta_{3D}\tilde{\psi}_{3D}(r)$, where $|\eta_{3D}|^2 = (1 + p^2a^2)^{-1}$ and p is the 3D relative momentum of colliding particles (see, e.g., [26]). Hence, for the inelastic rate constant we have $\langle \alpha_0(1 + p^2a^2)^{-1}\rangle$. In the presence of axial confinement, averaging the frequency of inelastic collisions over the (quantum) axial density profile $n_{3D}(z)$, we obtain

$$\Omega_{in} = \left\langle \frac{\alpha_0}{(1 + p^2a^2)} \right\rangle \int \frac{n_{3D}^2(z)}{n} dz. \tag{50}$$

The density profile $n_{3D}(z)$ accounts for the discrete structure of quantum levels in the axial confining potential and for the quantum spatial distribution of particles. Therefore, Eq. (50) gives the ordinary 3D result only at temperatures $T \gg \hbar\omega_0$, where $n_{3D}(z)$ becomes the Boltzmann distribution $n_B(z)$.

We first analyze the influence of axial confinement on Ω_{in} in Eq. (49) for the case where $|a| \ll \tilde{\Lambda}_T$ or, equivalently, $|a| \ll l_0$ and $q_T|a| \ll 1$. In this case we may put $\eta = 1$ at any T, except for extremely low temperatures in the quasi-2D regime. Then Eq. (49) gives

$$\Omega_{in} = \langle \varphi_\nu^2(0)\rangle \alpha_0 n = \frac{\alpha_0 n}{\sqrt{2\pi}\, l_0} \tanh^{1/2}\left(\frac{\hbar\omega_0}{T}\right). \tag{51}$$

One can easily check that Eq. (51) coincides with Eq. (50) in which $p|a| \ll 1$. The reason for this coincidence is that, similarly to the case of elastic scattering described by Eq. (29), for $\eta = 1$ the scattering amplitude f_{in} in Eq. (48) is independent of the relative energy ε. Hence, the inelastic rate is influenced by the axial confinement only through the axial distribution of particles. However, this influence is significant, in contrast to the case of elastic scattering under the same conditions [see Eq. (30)]. Qualitatively, for $q_T|a| \ll 1$ we have $\Omega_{in} \sim \alpha_0 n_{3D}$. At temperatures $T \ll \hbar\omega_0$, a characteristic value of the 3D density is $n_{3D} \sim n/l_0$ and we obtain $\Omega_{in} \sim \alpha_0 n/l_0$. For $T \gg \hbar\omega_0$, the 3D density $n_{3D} \sim n(m\omega_0^2/T)^{1/2}$ and hence the frequency of inelastic collisions is $\Omega_{in} \sim (\alpha_0 n/l_0)(\hbar\omega_0/T)^{1/2}$.

We now discuss the temperature dependence of the inelastic rate for the case where $|a| \gtrsim l_0$, which in the ultracold limit (9) assumes that $|a| \gg R_e$. In the quasi-2D regime and in the temperature interval $\varepsilon_* < T < \hbar\omega_0$ of the confinement-dominated 3D regime, the most important contribution to the inelastic rate in Eq. (49) comes from collisions with the axial quantum number $\nu = 0$. Then, using Eq. (18) we express the parameter η through the elastic amplitude f_{00} and obtain a relation between Ω_{in} and the mean frequency of elastic collisions $\Omega(T)$:

$$\Omega_{in}(T) = \langle |f_{00}(\varepsilon)|^2\rangle \frac{\alpha_0 n}{[4\pi a \varphi_0(0)]^2} = \Omega(T)\beta, \tag{52}$$

where $\beta = (1/128\pi^3)^{1/2}(ml_0\alpha_0/\hbar a^2)$ is a dimensionless parameter independent of temperature. The temperature dependence of Ω is displayed in Fig. 1 and Fig. 5 and was discussed in Secs. IV and V. Note that the parameter β is not equal to zero for $|a| \to \infty$. In this case, since the amplitude f_0 is calculated with the wave function $\tilde{\psi}_{3D}$ that behaves as a/r for $r \to \infty$, we have $\alpha_0 \propto a^2$ and $\beta = \text{const}$.

At temperatures $T \gg \hbar\omega_0$, using the same method as in Sec. V for the case of elastic scattering, from Eq. (49) we recover the 3D result Ω_{in}^{3D} given by Eq. (50) with $n_{3D}(z) = n_B(z)$. In the limiting case, where $q_T|a| \gg 1$, we find

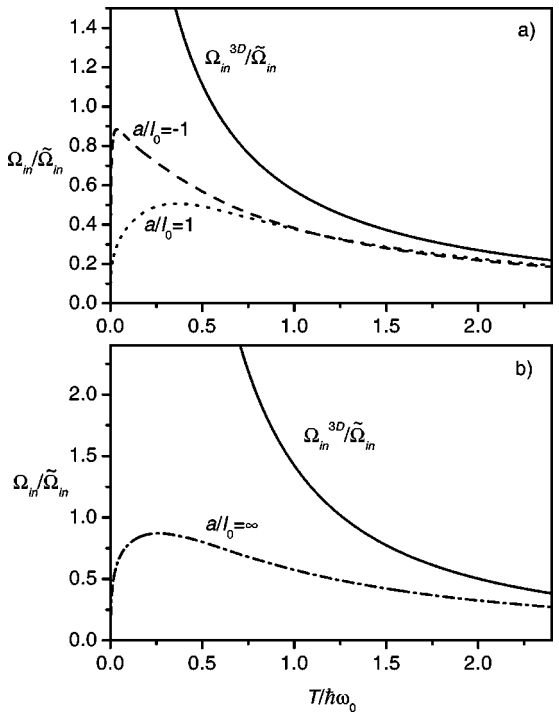

FIG. 7. The quantity $\Omega_{in}/\tilde{\Omega}_{in}$ versus $T/\hbar\omega_0$. In (a) the parameter $a/l_0=-1$ (dashed curve), and $a/l_0=1$ (dotted curve). In (b) $a/l_0=\infty$ (unitarity limit). The solid curves in (a) and (b) show the 3D result (52).

$$\Omega_{in}^{3D}=\frac{8\hbar n}{m}\beta\left(\frac{2\hbar\omega_0}{T}\right)^{3/2}=\Omega_{3D}(T)\beta\left(\frac{2\hbar\omega_0}{T}\right)^{1/2}. \quad (53)$$

Comparing Eq. (53) with Eq. (52), we see that in the confinement-dominated 3D regime the deviation of the inelastic rate from the ordinary 3D behavior should be larger than that in the case of elastic scattering.

As follows from Eq. (52) and Fig. 5, for $|a|\gtrsim l_0$ the inelastic frequency Ω_{in} reaches its maximum at temperatures near the border between the quasi-2D and confinement-dominated 3D regimes. The maximum value of Ω_{in} is close to

$$\tilde{\Omega}_{in}=\frac{16\hbar}{m}\beta. \quad (54)$$

From Eq. (49) one finds that at any T the ratio $\Omega_{in}/\tilde{\Omega}_{in}$ depends only on two parameters: $T/\hbar\omega_0$ and a/l_0. In Fig. 7 we present our numerical results for $\Omega_{in}/\tilde{\Omega}_{in}$ as a function of $T/\hbar\omega_0$ for a/l_0 equal to -1, 1, and ∞. As expected, the deviations from the 3D behavior are the largest in the unitarity limit.

The inelastic rate of spin relaxation in a tightly (axially) confined gas of atomic cesium has been measured for the unitarity limit in the Stanford experiment [6]. Due to a shallow radial confinement of the cloud in this experiment, the 2D density $n\sim 1/T$ [see Eq. (36)]. Then, Eq. (53) gives the 3D inelastic frequency $\Omega_{in}^{3D}\sim 1/T^{5/2}$, whereas in the temperature interval $\varepsilon_*<T<\hbar\omega_0$ of the confinement-dominated regime Eqs. (35) and (52) lead to $\Omega_{in}\sim(1/T)[1-\exp(-\hbar\omega_0/T)]$. In order to compare our calculations with the data of the Stanford experiment on spin relaxation, in Fig. 8 we display $\Omega_{in}(T)$ normalized to Ω_{in} at $T=3\hbar\omega_0$ that was the highest temperature in the experiment. The temperature dependence of the inelastic rate, following from the Stanford results, agrees fairly well with the calculations and shows significant deviations from the 3D behavior. It should be noted that, in contrast to thermalization rates, the inelastic decay rate is not sensitive to whether the gas is in the collisionless or hydrodynamic regime [6].

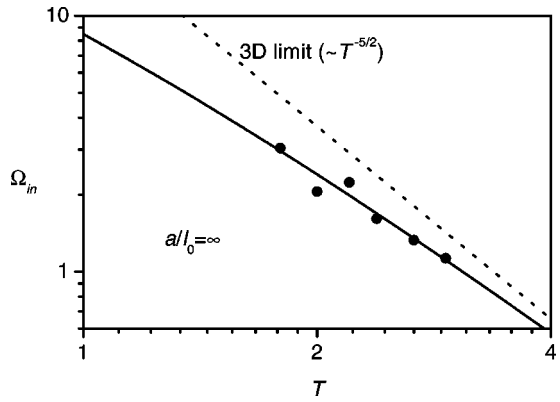

FIG. 8. Inelastic rate Ω_{in} normalized to Ω_{in} at $T=3\hbar\omega_0$, versus temperature (in units of $\hbar\omega_0$) in the unitarity limit ($a=\infty$). The solid curve shows the result of our numerical calculations, and the dotted line the 3D limit. Circles show the data of the Stanford experiment.

VIII. CONCLUDING REMARKS

In conclusion, we have developed a theory that describes the influence of a tight axial confinement of the particle motion on the processes of elastic and inelastic scattering. The most interesting case turns out to be the one in which the 3D scattering length a exceeds the extension of the wave function in the axial direction, l_0. In the ultracold limit defined by Eq. (9), the condition $|a|>l_0$ automatically requires large $|a|$ compared to the radius of interatomic interaction R_e. Then we have a pronounced confinement-dominated 3D regime of scattering at temperatures on the order of $\hbar\omega_0$. Treating interatomic collisions as three dimensional, the relative momentum of colliding atoms is related to the quantum character of the axial motion in the confining potential and becomes of the order of $1/l_0$. As a result, the scattering rate can strongly deviate from the ordinary 3D behavior. The axial extension of the wave function, achieved in the experiments at Stanford and ENS [5–8], is $l_0\approx 200$ Å. The required value of the scattering length, $|a|>l_0$ and $|a|\gg R_e$, is characteristic for Cs atoms ($R_e\approx 100$ Å) and can also be achieved for other alkali atoms by using Feshbach resonances.

In order to observe the 2D features of the particle motion in the rates of interatomic collisions one has to reach the quasi-2D regime of scattering, which requires much lower temperatures, at least by an order of magnitude smaller than $\hbar\omega_0$. For $\omega_0\approx 80$ kHz ($\hbar\omega_0\approx 4$ μK) as in the Stanford [5,6]

and ENS [7,8] experiments, these are temperatures below 400 nK. As one can see from Fig. 5, the rate of elastic collisions is still rather large for these temperatures and, hence, one can think of achieving them by evaporative cooling. Moreover, for realistic radial frequencies $\omega \sim 100$Hz there is a hope to achieve quantum degeneracy and observe a cross-over to the Bose-Einstein condensation (BEC) regime. The cross-over temperature is $T_c \approx N^{1/2}\hbar\omega$ (see [27] and the discussion in [9]), and for $N \sim 1000$ particles in a quasi-2D layer we find $T_c \approx 100$ nK.

Another approach to reach BEC in the quasi-2D regime will be to prepare initially a 3D trapped condensate and then adiabatically slowly turn on the tight axial confinement. Manipulating the obtained (quasi)2D condensate and inducing the appearance of thermal clouds with temperatures $T < T_c$, one can observe interesting phase coherence phenomena originating from the phase fluctuations of the condensate in quasi-2D (see [9]).

Interestingly, at temperatures $T \sim T_c$ the collisional frequency Ω can be on the order of the cross-over temperature if $|a| \gtrsim l_0$. This follows directly from Fig. 1 and Eq. (24) that give $\Omega \sim \pi\hbar n/m$ even at temperatures by two orders of magnitude smaller than $\hbar\omega_0$. As the 2D density of thermal particles is $n \sim Nm\omega^2/T$, we immediately obtain $\hbar\Omega(T_c) \sim N^{1/2}\hbar\omega \approx T_c$. This condition means that the trapped gas becomes a strongly interacting system. The mean free path of a particle $v/\Omega(T_c)$ is already on the order of its de Broglie wavelength $\hbar/\sqrt{mT_c}$. At the same time, the system remains dilute, since the mean interparticle separation is still much larger than the radius of interatomic interaction R_e. In this respect, the situation is similar to the 3D case with a large scattering length $a \gg R_e$ at densities where $na^3 \sim 1$. The investigation of the crossover to the BEC regime in such strongly interacting quasi-2D gases should bring in analogies with condensed matter systems or dense 2D gases. Well-known examples of dense 2D systems in which the Kosterlitz-Thouless phase transition [28] has been found experimentally, are monolayers of liquid helium [29] and the quasi-2D gas of atomic hydrogen on liquid-helium surface [30].

On the other hand, for $|a| \ll l_0$ the collisional frequency near the BEC crossover, $\Omega(T_c) \ll T_c/\hbar$, and the (quasi)2D gas remains weakly interacting. Then, the nature of the crossover is questionable (see [9]). Generally speaking, one can have both the ordinary BEC crossover like in an ideal trapped gas [27] and the Kosterlitz-Thouless type [28] of a crossover. We thus see that axially confined Bose gases in the quasi-2D regime are remarkable systems where by tuning a or l_0 one can modify the nature of the BEC crossover.

ACKNOWLEDGMENTS

We acknowledge fruitful discussions with I. Bouchoule, C. Salomon, A. J. Kerman, V. Vuletić, and J. T. M. Walraven. This work was financially supported by the Stichting voor Fundamenteel Onderzoek der Materie (FOM), by INTAS, and by the Russian Foundation for Basic Studies.

[1] J.T.M. Walraven, in *Fundamental Systems in Quantum Optics*, Proceedings of the Les Houches Summer School, Session LIII, edited by J. Dalibard, J.M. Raimond, and J. Zinn-Justin (Elsevier Science, Amsterdam, 1992).

[2] M.H. Anderson, J.R. Ensher, M.R. Matthews, C.E. Wieman, and E.A. Cornell, Science **269**, 198 (1995).

[3] K.B. Davis, M.-O. Mewes, M.R. Andrews, N.J. van Druten, D.S. Durfee, D.M. Kurn, and W. Ketterle, Phys. Rev. Lett. **75**, 3969 (1995).

[4] C.C. Bradley, C.A. Sackett, J.J. Tollett, and R.G. Hulet, Phys. Rev. Lett. **75**, 1687 (1995).

[5] V. Vuletić, C. Chin, A.J. Kerman, and S. Chu, Phys. Rev. Lett. **81**, 5768 (1998).

[6] V. Vuletić, A.J. Kerman, C. Chin, and S. Chu, Phys. Rev. Lett. **82**, 1406 (1999).

[7] I. Bouchoule, H. Perrin, A. Kuhn, M. Morinaga, and C. Salomon, Phys. Rev. A **59**, R8 (1999); M. Morinaga, I. Bouchoule, J.-C. Karam, and C. Salomon, Phys. Rev. Lett. **83**, 4037 (1999).

[8] I. Bouchoule, Ph.D. thesis, LKB ENS, Paris, 2000; I. Bouchoule, M. Morinaga, D. S. Petrov, and C. Salomon (unpublished).

[9] D.S. Petrov, M. Holzmann, and G.V. Shlyapnikov, Phys. Rev. Lett. **84**, 2551 (2000).

[10] E. Tiesinga, A.J. Moerdijk, B.J. Verhaar, and H.T.C. Stoof, Phys. Rev. A **46**, R1167 (1992); E. Tiesinga, B.J. Verhaar, and H.T.C. Stoof, *ibid.* **47**, 4114 (1993).

[11] S. Inouye, M.R. Andrews, J. Stenger, H.-J. Miesner, D.M. Stamper-Kurn, and W. Ketterle, Nature (London) **392**, 151 (1998); J. Stenger, S. Inouye, M.R. Andrews, H.-J. Miesner, D.M. Stamper-Kurn, and W. Ketterle, Phys. Rev. Lett. **82**, 2422 (1999).

[12] Ph. Courteille, R.S. Freeland, D.J. Heinzen, F.A. van Abeelen, and B.J. Verhaar, Phys. Rev. Lett. **81**, 69 (1998).

[13] V. Vuletić, C. Chin, A.J. Kerman, and S. Chu, Phys. Rev. Lett. **83**, 943 (1999); C. Chin, V. Vuletić, A.J. Kerman, and S. Chu, *ibid.* **85**, 2717 (2000).

[14] J.L. Roberts, N.R. Claussen, S.L. Cornish, and C.E. Wieman, Phys. Rev. Lett. **85**, 728 (2000); S.L. Cornish, N.R. Claussen, J.L. Roberts, E.A. Cornell, and C.E. Wieman, *ibid.* **85**, 1795 (2000).

[15] L.D. Landau and E.M. Lifshitz, *Quantum Mechanics* (Butterworth-Heinemann, Oxford, 1999).

[16] For interatomic potentials that have a shallow well (spin-polarized atomic hydrogen), the bound state with an exponentially small binding energy ε_0, characteristic for shallow 2D potential wells [15], does not exist due to the presence of a strong repulsive core [17]. For potentials with a deep well (alkali atoms) the situation is similar to that in 3D. There are many bound states and only accidentally one can encounter a very weakly bound s-level ($d_* \to \infty$). Thus, for realistic momenta of particles in ultracold gases we always have the inequality $qd_* \ll 1$.

[17] Yu. Kagan, G.V. Shlyapnikov, I.A. Vartan'yantz, and N.A. Glukhov, Pis'ma Zh. Eksp. Teor. Fiz. **35**, 386 (1982) [JETP Lett. **35**, 477 (1982)].

[18] This is easily established by comparing the relation for the vertex of elastic interaction, obtained to zero order in perturbation theory [19], with the expression for the scattering amplitude [15]. In the case of an inhomogeneous density profile one should replace μ by n_0, where n_0 is the coordinate-dependent condensate density.

[19] A.A. Abrikosov, L.P. Gorkov, and I.E. Dzialoshinski, *Methods of Quantum Field Theory in Statistical Physics* (Dover, New York, 1975).

[20] In [9] the coefficient B was put equal to unity.

[21] In the Stanford experiment [6] the unitarity limit for collisions between Cs atoms in the hyperfine state $F=3$, $m_F=3$ has been achieved by tuning the magnetic field to the Feshbach resonance at 30 G. In the ENS experiment [8] the magnetic field was very small. According to the recent calculations [22], this corresponds to a large and negative scattering length ($a \sim -1500$ Å) for collisions between Cs atoms in $F=3$ states. For the ENS axial frequency $\omega_0=80$ kHz we have $l_0 \approx 200$ Å. Hence, the ratio $|a|/l_0$ in this experiment was approximately equal to 7, which is already rather close to the unitarity limit.

[22] P.J. Leo, C.J. Williams, and P.S. Julienne, Phys. Rev. Lett. **85**, 2721 (2000).

[23] V. Vuletić (private communication).

[24] J. Weiner, V.S. Bagnato, S. Zilio, and P.S. Julienne, Rev. Mod. Phys. **71**, 1 (1999).

[25] A.S. Davydov, *Quantum Mechanics* (Pergamon, Oxford, 1976).

[26] P.O. Fedichev, M.W. Reynolds, U.M. Rahmanov, and G.V. Shlyapnikov, Phys. Rev. A **53**, 1447 (1996).

[27] V. Bagnato and D. Kleppner, Phys. Rev. A **44**, 7439 (1991).

[28] J.M. Kosterlitz and D.J. Thouless, J. Phys. C **6**, 1181 (1973); J.M. Kosterlitz, *ibid.* **7**, 1046 (1974).

[29] D.J. Bishop and J.D. Reppy, Phys. Rev. Lett. **40**, 1727 (1978); Phys. Rev. B **22**, 5171 (1980).

[30] A.I. Safonov, S.A. Vasilyev, I.S. Yasnikov, I.I. Lukashevich, and S. Jaakkola, Phys. Rev. Lett. **81**, 4545 (1998).